

Tuning Photoinduced Energy- and Electron-Transfer Events in Subphthalocyanine–Phthalocyanine Dyads

David González-Rodríguez,^[a] Christian G. Claessens,^[a] Tomas Torres,^{*[a]} Shenggao Liu,^[b] Luis Echegoyen,^{*[b]} Nuria Vila,^[c] and Santi Nonell^{*[c]}

In memoriam Dr. Juan Carlos del Amo, who died in the tragedy in Madrid on March 11th

Abstract: A series of subphthalocyanine–phthalocyanine dyads has been prepared by means of palladium-catalyzed cross-coupling reactions between a monoalkynylphthalocyanine and different monoiodosubphthalocyanines. Electronic coupling between the two photoactive units is ensured by a rigid and π -conjugated alkynyl spacer. In addition, the electronic characteristics of the subphthalocyanine moiety were modulated by the introduction of different peripheral substituents. Cyclic and Osteryoung square-wave voltammetry experiments revealed that the reduction potential of this subunit can be decreased by about 400 mV on

going from thioether or no substituents to nitro groups. As a consequence, the energy level of the charge-transfer state could be fine-tuned so as to gain control over the fate of the photoexcitation energy in each subunit. The diverse steady-state and time-resolved photophysical techniques employed demonstrated that, when the charge-transfer state lies high in energy, a quantitative singlet–singlet energy-

transfer mechanism from the excited subphthalocyanine to the phthalocyanine takes place. On the contrary, stabilization of the radical pair by lowering the redox gap between electron donor and acceptor results in a highly efficient photoinduced electron-transfer process, even in solvents of low polarity such as toluene ($\Phi_{ET} \approx 0.9$). These features, together with the extraordinary absorptive cross section that these molecular ensembles display across the whole UV/Vis spectrum, make them model candidates for application in situations where broadband light sources are needed.

Keywords: electrochemistry • electron transfer • photochemistry • phthalocyanines • subphthalocyanines

Introduction

In recent years, a great deal of research has aimed at the understanding of the mutual interplay between energy- and


electron-transfer processes in synthetic molecular or supramolecular systems^[1] designed to reproduce the fundamental energy exchanges occurring in natural photosynthesis.^[2] These systems are based on electron-donor and -acceptor

[a] Dr. D. González-Rodríguez, Dr. C. G. Claessens, Prof. T. Torres
Departamento de Química Orgánica (C-I)
Facultad de Ciencias, Universidad Autónoma de Madrid
Cantoblanco, 28049 Madrid (Spain)
Fax: (+34)91-497-3966
E-mail: tomas.torres@uam.es

[b] Dr. S. Liu, Prof. L. Echegoyen
Department of Chemistry
Clemson University, SC 29634 (USA)
Fax: (+1)864-656-6613
E-mail: luis@clemson.edu

[c] N. Vila, Prof. S. Nonell
Grup d'Enginyeria Molecular (GEM)
Institut Químic de Sarrià, Universitat Ramon Llull

Via Augusta 390, 08017 Barcelona (Spain)
Fax: (+34)93-205-6266
E-mail: s.nonell@iqs.url.edu

 Supporting information for this article is available on the WWW under <http://www.chemeurj.org/> or from the author: Selected ¹H NMR, ¹³C NMR, MS, and UV/Vis spectra of SubPcs **4a–d** and **5a–c**, Pcs **2** and **3**, and SubPc–Pc dyads **1a–c**, with complete assignment of NMR signals. Fluorescence emission, excitation, phosphorescence emission, and triplet–triplet absorption spectra of reference compounds **5a–c**, **3**, and dyads **1a–c**.

units linked by a well-defined spacer and thus mimick some aspects of the protein-embedded multiporphyrin–quinone assembly found in nature. Chemists, however, are not restricted to these natural components and, though extensive work has been dedicated to the study of porphyrin–quinone dyads,^[3] other photo- or electroactive moieties, which in some cases provide novel or enhanced properties,^[4] may be employed in such artificial photosynthetic systems.

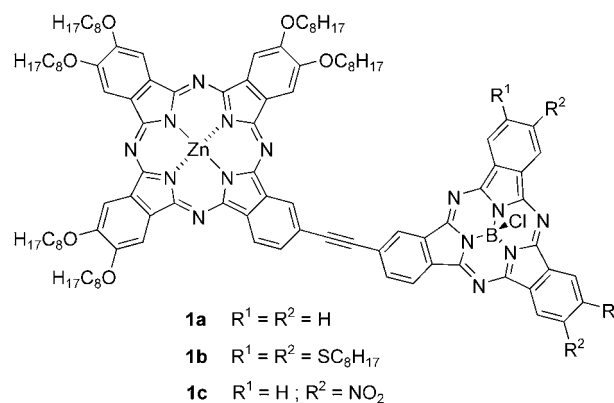
Phthalocyanines^[5] (Pcs) are 18 π -electron aromatic compounds made of four isoindole units linked together through their 1,3-positions by aza bridges. Two-dimensional aromatic delocalization over these macrocycles gives rise to their exceptional optical and electrical properties, which have found wide application in materials science.^[5b] Subphthalocyanines^[6] (SubPcs), lower homologues of phthalocyanines, are 14 π -electron aromatic compounds comprising three N-fused diiminoisoindole units. The C₃ aromatic structure and cone-shaped geometry of SubPcs makes them very promising candidates in the fields of supramolecular chemistry,^[7] nonlinear optics,^[8] and photo- or electroactive systems.^[9]

For these reasons, it is not surprising that many examples of SubPc- and Pc-containing dyads and triads have been described in the literature.^[9,10] Nonetheless, the study of the interchromophoric interactions, both in the ground and excit-

ed state, of covalently linked SubPc–Pc systems is still pending. Owing to the particular electronic properties of each of these units,^[5,8a,11] such an ensemble seems to be perfectly suited for the study of intramolecular energy/electron-transfer processes.^[12] First, since the absorption of each chromophore perfectly complements that of the other, a SubPc–Pc dyad would cover a very wide section (up to 750 nm) of the UV/Vis spectrum. Second, energy transfer from the higher lying SubPc singlet excited state (ca. 2.1 eV) to the Pc singlet (ca. 1.8 eV) seems a quite plausible deactivation pathway, whereby the SubPc plays the role of a light-harvesting antenna. Finally, the redox gradient can be easily tuned by the introduction of different peripheral substituents on both macrocycles, and thus control can be gained over the competition between photoinduced energy- and electron-transfer mechanisms.^[9b]

Here we describe the design and synthesis of a series of SubPc–Pc dyads **1a–1c**, as well as the study of their most relevant electrochemical and photophysical properties. The

Abstract in Spanish: *Se han preparado una serie de díadas de subftalocianina-ftalocianina a través de reacciones de acoplamiento cruzado catalizadas por paladio entre una monoalquilftalocianina y distintas monoiodosubftalocianinas. El empleo de un espaciador rígido y π -conjugado de tipo alquínico asegura el acoplamiento electrónico entre ambas unidades. Además, las características electrónicas de la unidad de subftalocianina han sido moduladas mediante la introducción de diferentes sustituyentes periféricos. De hecho, los experimentos de voltametría cíclica y de onda cuadrada de Osteryoung han revelado que el potencial de reducción de esta unidad puede disminuirse en aproximadamente 400 mV al ir desde sustituyentes tioéter o ningún sustituyente, a grupos nitro. Como consecuencia, el nivel de energía del estado de transferencia de carga puede ajustarse con el fin de alcanzar un control sobre el destino de la energía de fotoexcitación en cada subunidad. Las diversas técnicas fotofísicas empleadas han demostrado que, en aquellos casos en los que el estado de separación de cargas posee una energía elevada, se produce una transferencia de energía cuantitativa desde el estado singlete de la subftalocianina al singlete de la ftalocianina. Por el contrario, la estabilización del par radical mediante la disminución del gap redox entre el dador y el aceptor de electrones da lugar a un proceso de transferencia electrónica fotoinducida muy eficiente, incluso en disolventes de polaridad moderada como el tolueno ($\Phi_{ET} \sim 0.9$). Estas características, junto con la intensa absorción que presentan estas moléculas en todo el espectro de UV/Vis, las convierte en excelentes candidatos para su aplicación en aquellos casos en los que se necesiten fuentes de luz de banda ancha.*



two units are linked by a conjugated ethynyl spacer, which allows efficient electronic communication.^[12] The Pc fragment is equipped with solubilizing, electron-donating octyloxy groups, and variation of the peripheral substituents of the SubPc ring allows fine-tuning of its reduction potential and therefore of the energy level of the charge-transfer state, whose population may compete with energy-transfer mechanisms. The synthetic approach envisaged for SubPc–Pc dyads **1a–c** is centered on a palladium-mediated cross-coupling reaction between different monoiodo-SubPcs and a Pc bearing a single ethynyl group. The Pc and SubPc moieties were chosen so as to avoid the presence of a mixture of more than one isomer in a given dyad. This strategy therefore requires the isolation of specifically substituted macrocycles resulting from the statistical condensation of two different phthalonitriles. Even if the syntheses of such unsymmetrically substituted Pcs^[13] and SubPcs^[14] are now well documented, they still represent a challenge as far as purification is concerned. It is well known that strong aggregation of Pcs in solution usually makes their chromatographic separation a tedious process. Nonplanar SubPcs, in contrast, show a much lower tendency to aggregate and in most cases

even regioisomerically pure compounds can be isolated from these complex mixtures.^[14]

Results and Discussion

Synthesis and characterization: Pc **2** was synthesized in 14% yield by statistical condensation of 4,5-dioctyloxyphthalonitrile and 4-(3-hydroxy-3-methyl-1-butynyl)phthalonitrile in dimethylaminoethanol (DMAE) in the presence of zinc chloride (Scheme 1).^[15] The presence of a bulky dimethylcarbinol protecting group facilitated chromatographic separation of **2** from the other Pc derivatives formed. Deprotection of Pc **2** to give Pc **3** was achieved in 73% yield by treatment with NaOH in toluene.^[16] The stacking of these Pc macrocycles in solution produces broad features in the ¹H NMR spectra, especially those corresponding to the aromatic protons. In the case of Pc **2**, broad signals were detected between $\delta=7$ and 8 ppm and around $\delta=4$ ppm, corresponding to the aromatic and the OCH₂ protons, respectively. For Pc **3**, only the aliphatic part of the spectrum could be distinguished. Compounds **2** and **3** both exhibit the typical electronic transitions of Pcs (Figure 1a). From the relative widths and intensities of the Q band of both macrocycles (at 685 nm), it can be inferred that, at the same concentration, Pc **3** has a somewhat higher degree of aggregation in CHCl₃, which can be reduced by dilution. The IR features of both

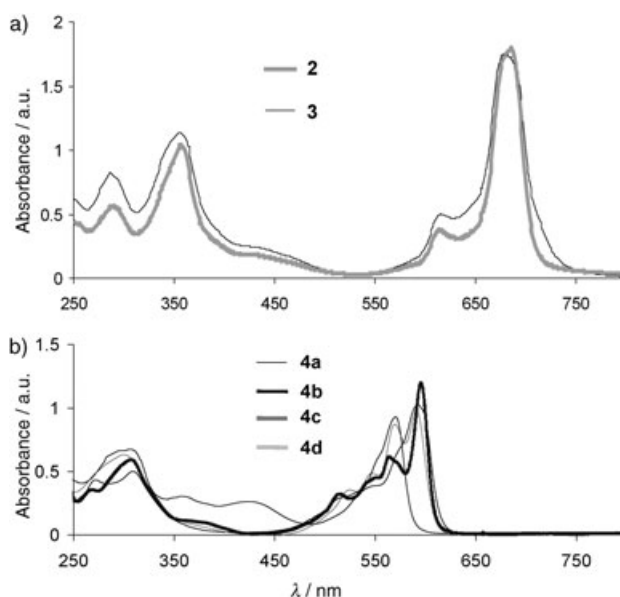
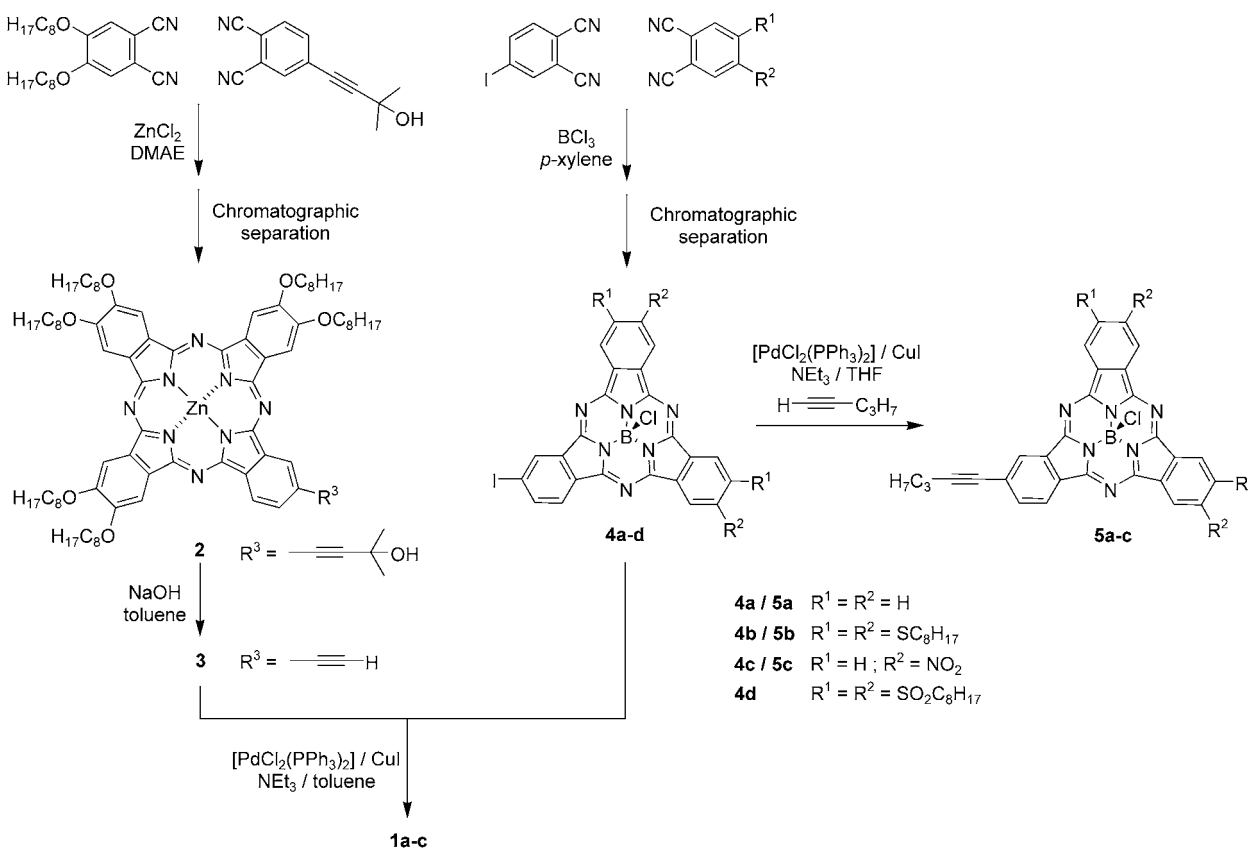


Figure 1. UV/Vis spectra (CHCl₃, 2.5 × 10⁻⁵ M) of a) Pcs **2** and **3** and b) SubPcs **4a–d**.

Pcs are very similar. However, in the case of Pc **3**, new bands at 3306 and 2110 cm⁻¹ were ascribed to the stretching of the alkynyl C–H and C≡C bonds, respectively.



Scheme 1. Synthesis of SubPc–Pc dyads **1a–c** and reference compounds SubPcs **4a–d**, **5a–c** and Pc **3**.

Monoiodo-SubPcs **4a–d** (Scheme 1) were likewise obtained by statistical condensation of the two corresponding phthalonitrile derivatives in the presence of boron trichloride in *p*-xylene at reflux.^[17] Most compounds and isomers could be isolated from the resulting reaction mixture by column chromatography on silica gel with appropriate eluents.^[18] Unlike Pcs, SubPcs yield quite informative NMR spectra, which helped in the identification of the desired isomers. The electronic absorption spectra of **4a–d** (Figure 1b) display the typical B and Q bands of SubPcs at around 300 and 580 nm, respectively. The latter presents a red shift with respect to unsubstituted SubPc, whose magnitude depends on the nature of the peripheral substituents and which is especially evident for SubPcs **4b–d**. A less intense band around 400 nm, attributed to $n \rightarrow \pi^*$ transitions, was also seen for **4b**.

SubPc–Pc dyads **1a**, **1b**, and **1c** were synthesized by standard Sonogoshira palladium cross-coupling with iodo-SubPcs **4a**, **4b**, and **4c**, respectively, in the presence of catalytic amounts of $[\text{PdCl}_2(\text{PPh}_3)_2]$ and CuI. Dry and deoxygenated solvents (toluene or THF) must be utilized to minimize formation of the bis-phthalocyanine derivative from **3** by oxidative homocoupling.^[19] Notwithstanding this drawback, the Pc dimer is formed in the very first steps of the mechanism to generate the active catalytic species (Pd^0). Therefore, the addition of a small excess of Pc **3** (1.2 equiv) was found to be essential for total SubPc consumption, which was monitored by TLC. A remarkable dependence of the reaction rate on SubPc peripheral substitution was noticed; electron-poor aromatic rings react much faster (**4c** > **4a** > **4b**). Compound **4d**, bearing alkylsulfonyl functional groups, could not be coupled under these conditions, and instantaneous decomposition was observed instead. In fact, the addition of triethylamine to toluene or THF solutions of **4d** resulted in the total bleaching of the original pink color. The use of other bases (diisopropylethylamine, 1,8-diazabicyclo[5.4.0]undec-7-ene) or lower temperatures reproduced qualitatively the same outcome. After chromatographic separation, dyads **1a** (dark blue solid), **1b** (green viscous solid), and **1c** (green-blue solid) were obtained in 53, 45, and 69% yield, respectively. In all cases, the bis-Pc by-product was isolated in 5–10% yield. The three dyads are very soluble in common organic solvents and were characterized by ^1H NMR, IR, UV/Vis, MALDI-TOF MS, and elemental analysis. Similar to Pcs, the ^1H NMR spectra of **1a–c** show very broad signals, but those corresponding to the OCH_2 and SCH_2 (for **1b**) protons could be clearly recognized. MALDI-TOF MS experiments revealed the molecular ion of **1a–c** as the most prominent peak, with an isotopic pattern that compares well with the simulated one (see Supporting Information).

Pentynyl-substituted SubPcs **5a**, **5b** and **5c** were synthesized as test compounds in 78, 54, and 88% yield, respectively, according to the same cross-coupling methodology starting from 1-pentyne and iodo-SubPcs **4a**, **4b**, and **4c**. In this reaction, precursors **4a–c** followed the same reactivity pattern aforementioned for the synthesis of the dyads, that

is, electron-deficient macrocycles reacted faster. Once more, SubPc **4d** did not lead to the expected coupling compound but decomposed on addition of the base. The characterization of **5a–c** by ^1H and ^{13}C NMR, IR, UV/Vis, FAB-MS, and elemental analysis confirmed the presence of the 1-pentynyl group in the periphery of the macrocycle.

Electrochemistry: The solution electrochemistry of SubPc–Pc dyads **1a–c** was studied by cyclic voltammetry (CV) and Osteryoung square-wave voltammetry (OSWV) in dry THF and *o*-dichlorobenzene (*o*-DCB). The results measured for the dyads were compared with those of reference Pc **3** and SubPcs **4a–c**. The CVs and OSWVs are presented in Figures 2 and 3, respectively. The OSWV peak potentials are collected in Table 1.

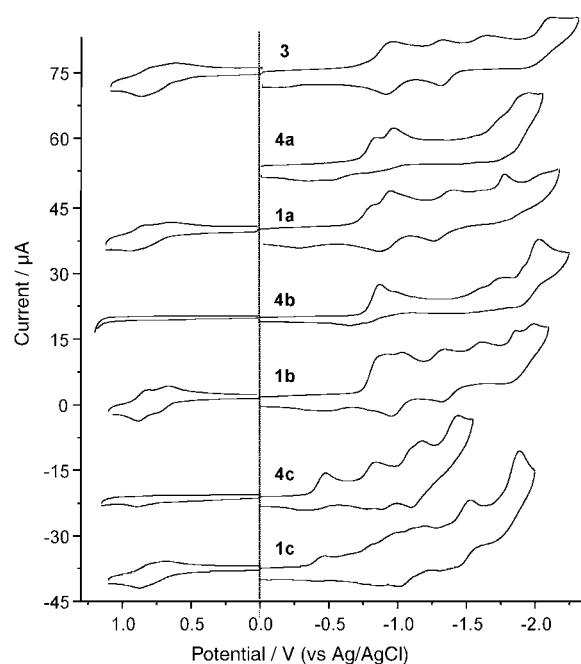


Figure 2. Cyclic voltammograms (sweep rate 0.1 V s^{-1}) for dyads **1a–c**, SubPcs **4a–c**, and Pc **3** in THF/TBAPF₆ at room temperature.

Model Pc **3** exhibits two hardly resolvable one-electron quasireversible oxidation waves on the CV anodic scan in THF. The resolution of the oxidation waves was not improved by changing the scan rate and the solvent (*o*-DCB). In this aromatic solvent, the oxidation waves became slightly less resolved than in THF. This indicates that the ZnPc compound shows a slightly higher tendency toward aggregation in *o*-DCB than in THF, which is in agreement with our own recent experience.^[10h] Because the anodic scan window is much wider in *o*-DCB (0–1.5 V) than in THF (0–1.1 V), we observed in this solvent a second oxidation wave around 1.3 V, which could be attributed to a third oxidation of the Pc ring or the oxidation of nitrogen in the Pc unit. In the cathodic scan, Pc **3** showed four electrochemically quasi-

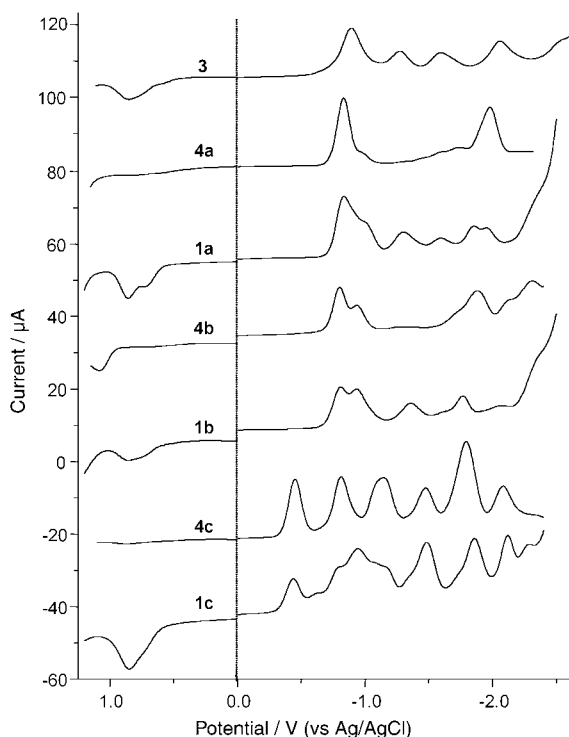


Figure 3. Oxidative and reductive OSWVs for dyads **1a–c**, SubPcs **4a–c**, and Pc **3** in THF/TBAPF₆ at room temperature.

reversible processes in THF between 0 and -2.3 V (see Table 1).

In the CVs of SubPc reference compounds **4a** and **4c**, no macrocycle-based anodic waves were observed between 0 and $+1.2$ V in THF, while for **4b** an oxidation wave was seen at 1081 mV in the OSWV. In contrast, in the cathodic part of the voltammograms, these compounds displayed a very rich electrochemistry, with the first reductive event at -832 (**4a**), -801 (**4b**), and -452 mV (**4c**). The reversibility of this first cathodic wave was found to be greatly dependent on the scan rate. Thus, for example, increasing the scan rate to 600 mV s^{-1} for **4a** made this wave chemically reversible but electrochemically irreversible with $\Delta E_p = 110$ mV. The electron-withdrawing effect of the nitro groups is not only reflected in the lower reduction potentials, but also in the larger number of reductive processes observed (six pronounced waves from -0.4 to -2.4 V, see Table 1). Other

weak reductions were observed for **4a** and **4b** that may be due to decomposition products or impurities.

The voltammograms of SubPc–Pc dyads show some features in common with their individual subunits. Owing to the large number of redox processes, their assignment to each electroactive component was achieved on the basis of their OSWVs, which show more clearly resolved waves (Figure 3). In the anodic part of the OSWVs in THF it is clear that, after covalent bonding to the SubPc moiety in the dyads, the Pc-based oxidations became more resolvable under identical experimental conditions. This may indicate intramolecular electronic interactions between the two components or a lower degree of Pc ring stacking on the attachment of the nonplanar SubPc. In the cathodic sweep direction, the origin of the reduction processes was assigned to one or other electroactive component (see Table 1). The assignment was facilitated by the difference in reversibility that the waves of each moiety exhibited. For instance, one can assign that the first reduction of **1a** to the SubPc unit, since this reduction peak becomes chemically more reversible at higher scan rates, as in the case of **4a**. On sweeping to highly negative potentials (> -1.5 V) several waves were observed, but most of them could not be assigned to either of the subunits.

The electrochemical data collected in Table 1 show that the redox potentials of both the Pc and SubPc moieties in dyads **1a–c** changed to some extent compared to those of model compounds **3** and **4a–c**, and this indicates some degree of intramolecular electronic interaction between the two fragments in the ground and/or charged states. Thus, for example, when we carefully compare the redox potentials of **3**, **1a**, and **4a**, we find that the first Pc-based oxidation and reduction potentials are both slightly negatively shifted in the dyad by 30 and 100 mV, respectively. Similar negative shifts were also observed for **1b** and **1c**.

Photochemistry: The properties of the excited states of dyads **1a–c** were analyzed by means of different photophysical techniques and compared to those of reference compounds **3** and **5a–c**. The most relevant photophysical data are collected in Table 2.

First, the steady-state absorption and emission spectra of the three dyads and their individual components in various solvents were compared. Aggregation phenomena, especially evident for dyad **1c**, were detected in CHCl_3 , toluene, and

Table 1. Electrochemical data [mV versus Ag/AgCl] of the redox processes of dyads **1a–c**, SubPcs **4a–c** and Pc **3** detected by OSWV in THF solution at room temperature under identical experimental conditions. Errors are estimated at about ± 5 mV.

	E_{ox}^3	E_{ox}^2	E_{ox}^1	E_{red}^1	E_{red}^2	E_{red}^3	E_{red}^4	E_{red}^5	E_{red}^6	E_{red}^7	E_{red}^8	E_{red}^9
3		840	750 ^[a]	−904	−1288	−1604	−2068	−2557				
4a				−832	−1980							
1a		856 ^[P]	720 ^[P]	−832 ^[S]	−1002 ^[P]	−1300 ^[P]	−1592 ^[P]	−1855 ^[P/S]	−1955 ^[P/S]			
4b			1081	−801	−934	−1881	−2313					
1b	> 1200 ^[S]	856 ^[P]	740 ^{[a][P]}	−814 ^[S]	−933 ^{[2c][P/S]}	−1364 ^[P]	−1769 ^[P]	−2066 ^[P/S]	−2365 ^[P/S]			
4c				−452	−812	−1144	−1476	−1795	−2083			
1c		848 ^[P]	740 ^{[a][P]}	−437 ^[S]	−799 ^[S]	−944 ^[P]	−1080 ^[S]	−1161 ^[P/S]	−1486 ^[P/S]	−1858 ^[P/S]	−2120 ^[P/S]	−2287 ^[P/S]

[a] Hardly resolved process, shoulder value: [P] = Pc-based redox processes; [S] = SubPc-based redox processes; [P/S] = not assignable.

Table 2. Summary of photophysical data acquired for SubPc-Pc dyads **1a–c** and reference Pc **3** and SubPcs **5a–c** in toluene/pyridine (25/1), unless otherwise specified.

	λ_{exc} [nm]	5a	5b	5c	3	1a	1b	1c
λ_{max} [nm]		573 (4.5)	595 (4.6)	596 (4.6)	686 (4.9)	698 (4.8)	701 (4.9)	702 (4.9)
$(\lg \epsilon)^{[a]}$				573 (4.5)		677 (4.8)	677 (4.9)	678 (5.0)
E_{Singlet} [eV] ^[b]		2.16	2.06	2.06	1.81	578 (4.5)	597 (4.6)	594 (4.6)
Φ_{F} ^[b]	570	0.51	0.39	0.47	–	0.20 ^[P]	0.19 ^[P]	0.02 ^[P] /0.002 ^[c,P]
	640	–	–	–	0.20	0.005 ^[S]	0.005 ^[S]	0.003 ^[S] /0.003 ^[c,S]
τ_{S} [ns]	590	3.1	2.8	3.3	–	0.19 ^[P]	0.19 ^[P]	0.04 ^[P] /0.01 ^[c,P]
	370	–	–	–	3.1	2.7	3.0	to assign
E_{Triplet} [eV] ^[b]		– ^[d]	– ^[d]	– ^[d]	1.12	1.11 ^[P]	1.11 ^[P]	– ^[d]
k_{F} [10^8 s^{-1}]	–	1.6	1.4	1.6	0.65	–	–	–
Φ_{Δ}	570	0.59	0.61	0.46	–	0.55	0.50	0.059
	646	–	–	–	0.54	0.55	0.56	0.15
τ_{T} [μs]	570	90	120	85	–	79	107	not detected
	640	–	–	–	110	100	118	110
ΔG_{CT} [eV] ^[e]						toluene: 2.14	toluene: 2.17	toluene: 1.73
						CH_2Cl_2 : 1.39	CH_2Cl_2 : 1.42	CH_2Cl_2 : 0.99
Φ_{EN}	570					1.00 ± 0.01	1.00 ± 0.01	0.39 ± 0.01
k_{EN} [10^{10} s^{-1}]						3 ± 1	3 ± 1	3 ± 1
Φ_{ET}	570					–	–	0.9 ± 0.1 ^[f]
	640					–	–	0.75 ± 0.05
k_{ET} [10^{10} s^{-1}]						–	–	5 ± 1 ^[S] /0.1 ^[P]

[a] Only the Q band absorption maxima (in CHCl_3) of both chromophores are given. [b] For dyads **1a–c**: [P]=values assigned to a Pc excited state; [S]=values assigned to a SubPc excited state. [c] In toluene/ CH_2Cl_2 (4/1). [d] Phosphorescence was not detected. [e] Free energy level of the charge-transfer state calculated as described in the Experimental Section. [f] Total electron-transfer quantum yield, obtained from the contributions of both SubPc and Pc singlet excited states.

cyclohexane/pyridine by a concentration-dependent broadening of the Q band of the Pc and reduction of its intensity (see Supporting Information). In contrast, THF and toluene/pyridine (25/1) were found to impede ring stacking, since the spectra measured at different chromophore concentrations were virtually identical in the range 10^{-7} to 10^{-4} M. In all cases, though the individual contributions of the SubPc and Pc to the electronic spectra of the dyads can be clearly recognized, the spectra are not merely the sum of the spectra of their macrocyclic components. As shown in Figure 4, a small but clear bathochromic shift in both Q bands as well as a more pronounced splitting of the Pc Q band is observed, which indicates that π conjugation is extended through the triple bond and confirms electronic communication between the two macrocycles.^[10a] The absorption of these SubPc–Pc ensembles covers a huge range of the UV/

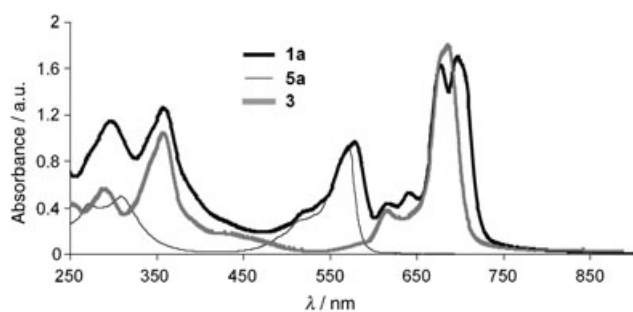


Figure 4. UV/Vis spectra (CHCl_3 , 2.5×10^{-5} M) of SubPc–Pc dyad **1a** and reference compounds **3** and **5a**.

Vis spectrum (up to 750 nm),^[20] since each individual chromophore fills regions of low absorption of the other.

In steady-state fluorescence experiments, the wavelength gap between the Q bands of the two chromophores (> 100 nm) allowed the selective excitation of each macrocycle. Each sample was accordingly irradiated at two different wavelengths: 570 nm, where most of the radiation is absorbed by the SubPc unit, and 640 nm, where only the Pc is able to absorb. Excitation at the blue edge of the absorption bands was mandatory to avoid Rayleigh scattering overlapping the fluorescence. Figure 5 displays the absorption and emission spectra of **1b** in toluene/pyridine (25/1) as an example. For dyads **1a** and **1b**, in which the SubPc moiety bears no substituents or thioether groups, excitation of either of the two units led to the detection of a major emission band with a maximum at 710 nm. These features, which match the fluorescence signal of **3**, are consistent with the emission of the Pc component. An additional very weak band centered around 600 nm, corresponding to the SubPc fluorescence emission, can also be distinguished when exciting at 570 nm.

Fluorescence quantum yields of **1a** and **1b** were then measured to quantify the singlet emission from the Pc at both wavelengths. As reference compounds, zinc phthalocyanine (ZnPc, $\Phi_{\text{F}}=0.30$)^[21] was used for $\lambda_{\text{exc}}=640$ nm, and subnaphthalocyanine ($\Phi_{\text{F}}=0.22$)^[11c] was employed at $\lambda_{\text{exc}}=570$ nm. Interestingly, the fluorescence quantum yields determined ($\Phi_{\text{F}}=0.19 \pm 0.01$) were exactly the same in the two dyads and for the two excitation wavelengths, as well as being identical to that obtained for reference Pc **3** (see

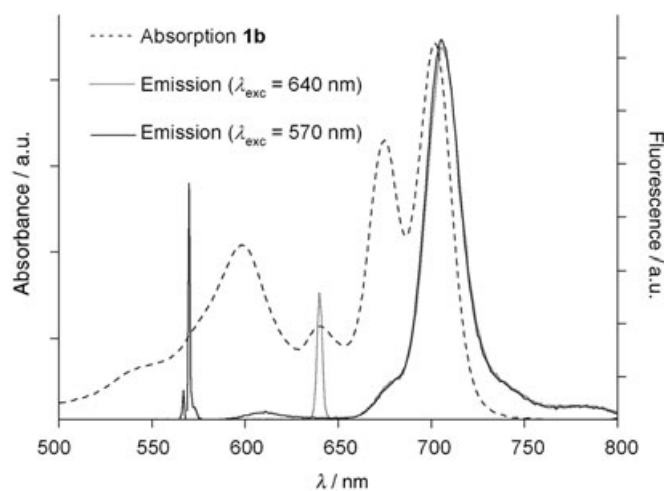


Figure 5. Absorption and emission spectra (excitation at 570 and 640 nm) of dyad **1b** in toluene/pyridine (25/1).

Table 2). On the other hand, fluorescence quantum yields of the SubPc unit in **1a** and **1b** were estimated to be less than 0.005 by using cresyl violet in methanol as reference ($\Phi_F = 0.54$),^[22] much lower than those of references **5a–c** ($\Phi_F = 0.39–0.51$). Given the energy values for the singlet excited state of both subunits (ca. 2.1 eV for SubPc and 1.7 eV for Pc) and the fact that excitation at 570 nm mainly (>90%) populates the singlet SubPc, this outcome points to an efficient energy-transfer process from the excited SubPc unit to the Pc. Further evidence for energy transfer was obtained from the excitation spectra of dyads **1a** and **1b** (Figure 6). The excitation spectra of **1a** and **1b** are essentially coincident with the ground-state absorption spectra and revealing contributions from both chromophoric subunits.

The quantum yield of the energy-transfer process Φ_{EN} can be calculated from the fluorescence quantum yields of the dyads when selectively exciting the SubPc [$\Phi_F(570\text{ nm})$] and the Pc [$\Phi_F(640\text{ nm})$] by Equation (1).

$$\Phi_F(570\text{ nm}) = \Phi_F(640\text{ nm})\Phi_{EN} \quad (1)$$

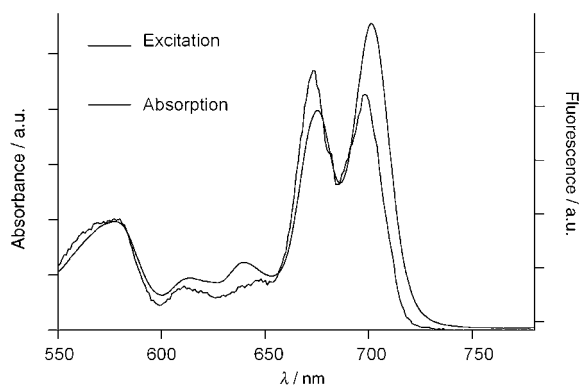


Figure 6. Absorption and excitation spectra of **1a** in toluene/pyridine (25/1); $\lambda_{\text{obs}} = 707\text{ nm}$.

In toluene/pyridine (25/1), $\Phi_F(570\text{ nm}) = \Phi_F(640\text{ nm}) = 0.19 \pm 0.01$; hence, the energy-transfer yield for **1a** and **1b** is $\Phi_{EN} = 1 \pm 0.01$. In addition, the fact that the fluorescence quantum yields coincide with that of the reference Pc rules out different deactivation pathways for the Pc-localized singlet excited state of the dyad than for the singlet of **3**. Quantitative energy-transfer events have also been observed in carotenoid–Pc^[10a] and porphyrin–Pc dyads.^[12]

A very different scenario was noted for compound **1c**, in which the SubPc unit is substituted with nitro groups. In this case, the emission and excitation spectra were strongly dependent on the solvent employed and, most importantly, fluorescence emission from both the SubPc and Pc components was substantially quenched (see Supporting Information). The magnitude of this quenching was found to be dependent on solvent polarity. For example, exciting the Pc unit ($\lambda_{\text{exc}} = 640\text{ nm}$) in toluene/pyridine (25/1) or in the more polar toluene/ CH_2Cl_2 (4/1) resulted in Pc-based fluorescence quantum yields of $\Phi_F = 0.04$ and 0.01, respectively. Exciting the SubPc moiety in both solvents resulted in the same trend, though the smaller fluorescence quantum yields of the Pc unit (see Table 2) indicate a less efficient energy-transfer process for dyad **1c**. On the other hand, the SubPc-based fluorescence yields were also slightly lower than in **1a** and **1b** ($\Phi_F \approx 0.003$ in both solvents). So, it seems that for dyad **1c** the singlet excited states of both units undergo a new nonradiative deactivation process, different from compounds **1a** and **1b**, which will be detailed below.

The fluorescence lifetimes of **1a–c** were determined by the time-correlated single-photon counting technique and are listed in Table 2 together with those of the model compounds. As in steady-state fluorescence experiments, the samples were irradiated at two different wavelengths to preferentially excite the SubPc ($\lambda_{\text{exc}} = 580$ or 590 nm) or the Pc moiety ($\lambda_{\text{exc}} = 370\text{ nm}$). In each test, the detection wavelength was set at 710 nm, the maximum of the Pc emission, or at 590 nm, the maximum of the SubPc emission. A singlet excited-state lifetime of about 3 ns was observed for the Pc moieties of **1a** and **1b**, a value which is similar to that found for reference compound **3** and for other zinc alkyloxyphthalocyanines^[23] and thus confirms the absence of additional deactivation pathways for the singlet Pc moiety in these dyads. While SubPcs **5a–c** are strongly fluorescent with singlet lifetimes of $\tau_s^0 = 2.8–3.3\text{ ns}$, our failure to observe any decay at their emission maximum in the dyads probably reflects a SubPc singlet lifetime close to or below the resolution limit of the apparatus used (ca. 30 ps). In fact, from the SubPc-based fluorescence yields and the lifetime of the model SubPcs, the singlet SubPc lifetime in dyads **1a**, **1b**, and **1c** is estimated as 30, 36, and 21 ps, respectively, by using Equation (2).

$$\Phi_F^0 / \Phi_F = \tau_s^0 / \tau_s \quad (2)$$

Likewise, we estimate the rate constant for energy transfer k_{EN} using Equation (3).

$$\Phi_F^0/\Phi_F = 1 + k_{EN} \cdot \tau_S^0 \quad (3)$$

A value of $k_{EN} = 3 \times 10^{10} \text{ s}^{-1}$ was obtained for dyads **1a** and **1b**. The rather complex fluorescence decay kinetics of dyad **1c** prevented assignment of the singlet lifetime in this system. We note, however, that the average lifetime is shorter than that of dyads **1a** and **1b**.

The energy of the triplet states of **1a–c** was elucidated from the near-IR room-temperature phosphorescence emission spectrum determined in laser flash photolysis experiments. Figure 7 illustrates the weak features recorded and their kinetic decay. Disappearance of the signal in the presence of oxygen confirmed the assignment to triplet phosphorescence. Triplet energies and phosphorescence lifetimes τ_p thus acquired for dyads **1a** and **1b** resembled those obtained for Pc **3** ($E_T = 1.11 \text{ eV}$ and $\tau_p = 60 \pm 5 \mu\text{s}$). In the case of dyad **1c**, phosphorescence that was too weak to be detected, which indicated lower population of the Pc triplet excited state.

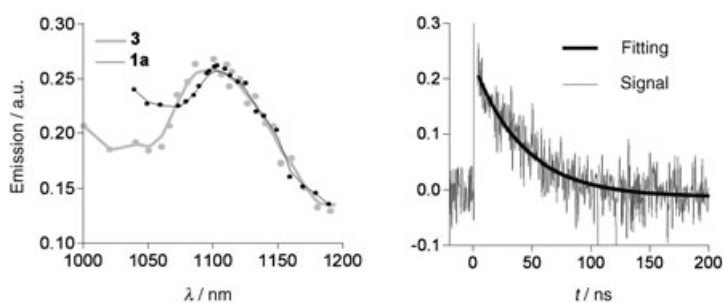


Figure 7. Phosphorescence emission spectra ($\lambda_{exc} = 650 \text{ nm}$) of dyad **1a** and Pc **3** and the corresponding decay signal ($\lambda_{obs} = 1100 \text{ nm}$) of dyad **1a** in argon-saturated toluene pyridine (25/1) at room temperature. The same spectrum was found for dyad **1b**.

Triplet quantum yields were not calculated, but a lower limit for this parameter can be estimated from measurements of singlet-oxygen production. For the determination of singlet-oxygen quantum yields Φ_{Δ} , the dyads were irradiated at two wavelengths and compared with a suitable reference compound: 1) for the selective excitation of the SubPc, the samples were irradiated at 570 nm and C_{60} ($\Phi_{\Delta} = 0.95$)^[24] was used as the reference, and 2) for the direct excitation of the Pc unit, irradiation was performed at 646 nm and tetraphenylporphyrin ($\Phi_{\Delta} = 0.62$)^[21] was used as reference compound. The data obtained in these experiments are included in Table 2.

Production of the triplet state was confirmed by time-resolved transient absorption measurements. The triplet–triplet absorption features of deoxygenated solutions of **1a–c** in toluene/pyridine (25/1) were determined and compared to the features of **3** and **5a–c**. Again, the samples were excited at 570 and 640 nm. The transient spectra registered (Figure 8), which match the triplet–triplet features of Pc **3** (see Supporting Information), were exactly the same at both excitation wavelengths and for the three dyads, even though

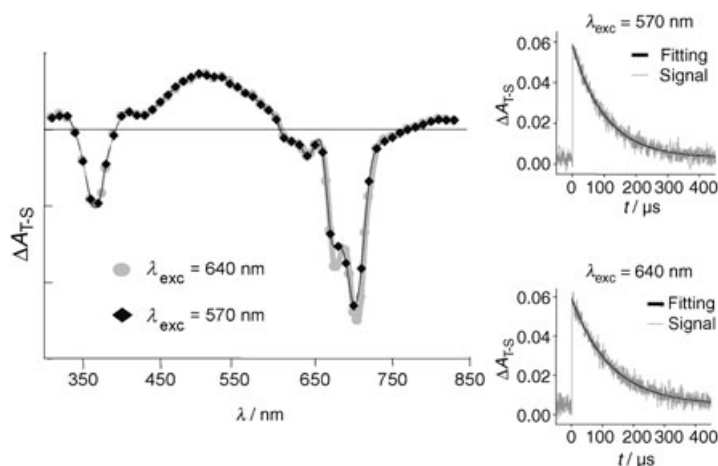


Figure 8. Left: Triplet–triplet transient absorption spectra of compound **1b** in argon-saturated toluene/pyridine (25/1). Right: Decay signals at 500 nm (excitation at 570 or 640 nm).

1c exhibited weaker signals that reflect a lower triplet quantum yield. In all cases, the signal grew with the time constant of our detection system (ca. 20 ns). Triplet-state lifetimes τ_T were deduced from the analysis of the transient decay kinetics (Figure 9) and are compiled in Table 2. Monoexponential decays were recorded for all compounds and at all excitation wavelengths, so the transient should be the product of only one triplet species that, in view of the similarity in spectral features and lifetimes, is assigned to the Pc triplet. No additional transients could be observed within the time resolution of our apparatus.

The outcome of these experiments (singlet-oxygen generation and time-resolved flash photolysis) further confirmed the conclusions drawn from steady-state and time-resolved fluorescence tests. First, an efficient singlet–singlet energy-transfer event from the SubPc to the Pc unit indeed occurs in **1a** and **1b**, since the spectral features and photophysical parameters derived ($\Phi_{\Delta} = 0.55 \pm 0.05$ and $\tau_T = 100 \pm 20 \mu\text{s}$) are very similar regardless of the excitation wavelength and equal to those of **3** ($\Phi_{\Delta} = 0.54$ and $\tau_T = 110 \mu\text{s}$). Figure 9 summarizes the deactivation route in dyads **1a** and **1b** on photoexcitation of the SubPc or the Pc component. First, because of the near 100% efficiency of energy transfer, these dyads can be said to behave photophysically as phthalocyanines, the only difference being that **1a** and **1b** maintain a strong absorption across almost the whole UV/Vis spectrum, whereby the SubPc antenna assists in the collection of electromagnetic radiation in the region below 600 nm.

Second, the Pc-based triplet undergoes no other process than decay to the ground state or, in the presence of oxygen, energy transfer to this species to produce singlet oxygen. Dyads **1a** and **1b** can thus be used as singlet-oxygen photosensitisers working throughout the UV and visible regions with wavelength-independent quantum yield. This feature endows SubPc–Pc dyads with ideal properties for application in situations where broadband light sources are used, for example, in solar photoreactors.

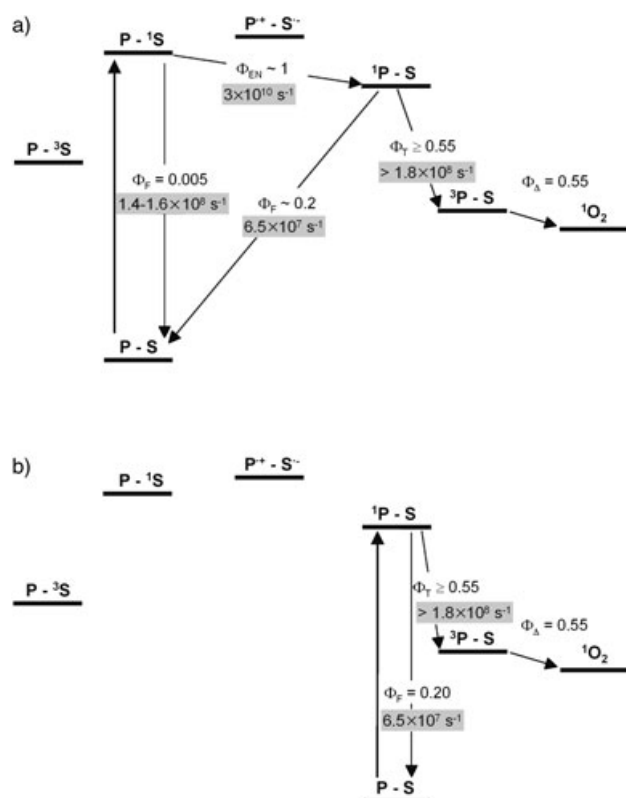


Figure 9. Photophysical processes occurring on a) SubPc or b) Pc excitation of SubPc-Pc dyads **1a** and **1b** in toluene/pyridine (25/1).

Third, a different deactivation route must be taking place in dyad **1c**, as the fluorescence and singlet-oxygen quantum yields are considerably lower and dependent on the direct excitation of the SubPc or the Pc. Interestingly, compound **1c** has the lowest reduction potential of the three dyads owing to the presence of electron-withdrawing nitro groups in the periphery of the SubPc macrocycle. Taking into consideration this fact, together with the high sensitivity of the fluorescence to the polarity of the medium, the most reasonable hypothesis for the deactivation of the singlet state of both subunits is the formation of a radical ion pair (SubPc^{•-}-Pc^{•+}) by electron transfer from the Pc to the SubPc. An approximate free energy of the charge-transfer state relative to the ground state ΔG_{CT} of **1a-c** in toluene and CH₂Cl₂ can be obtained from the first oxidation and reduction potentials in THF with consideration of solvent and distance effects (see Experimental Section). As can be noted from Table 2, only dyad **1c** has a charge-transfer state lower in energy than the singlet excited state of both chromophore subunits in toluene.

In the specific case of **1c**, the efficiency of singlet-singlet energy transfer Φ_{EN} can be estimated from the ratio of the fluorescence Φ_F or singlet-oxygen quantum yields Φ_Δ obtained for the Pc unit when exciting the SubPc ($\lambda_{exc} = 570 \text{ nm}$) or the Pc component ($\lambda_{exc} \approx 640 \text{ nm}$) [Eqs. (4) and (5)].

$$\Phi_{EN} = \Phi_F(\text{Pc}, \lambda_{exc} = 640 \text{ nm}) / \Phi_F(\text{Pc}, \lambda_{exc} = 570 \text{ nm}) \quad (4)$$

$$\Phi_{EN} = \Phi_\Delta(\text{Pc}, \lambda_{exc} = 646 \text{ nm}) / \Phi_\Delta(\text{Pc}, \lambda_{exc} = 570 \text{ nm}) \quad (5)$$

Values obtained in toluene/pyridine (25/1) are $\Phi_{EN} = 0.50 \pm 0.1$ and $\Phi_{EN} = 0.39 \pm 0.05$, respectively. Since Φ_F values have larger errors than Φ_Δ values, an energy transfer efficiency of 39% was assumed for **1c**, significantly lower than for dyads **1a** and **1b** (100% efficiency). Under the assumption that electron transfer accounts for this difference and since the sum of the yields of all pathways leading to the deactivation of the singlet excited state of the SubPc in **1c** must equal unity, an estimation of the electron transfer efficiency from the excited SubPc unit of $\Phi_{ET}(\text{SubPc}) = 0.61 \pm 0.05$ can be made. Combining this value with the yield and rate constant of energy transfer, the rate constant of electron-transfer from the singlet SubPc is estimated as $k_{ET} = 5 \times 10^{10} \text{ s}^{-1}$.

Similarly, the yield of the electron-transfer process from the Pc component $\Phi_{ET}(\text{Pc})$ can be approximated from the fluorescence or singlet-oxygen quantum yields of dyad **1c** and dyads **1a** or **1b** by means of the Equations (6) and (7).

$$\Phi_{ET}(\text{Pc}) = [\Phi_F(\mathbf{1a,1b}) - \Phi_F(\mathbf{1c})] / \Phi_F(\mathbf{1a,1b}) \quad (6)$$

$$\Phi_{ET}(\text{Pc}) = [\Phi_\Delta(\mathbf{1a,1b}) - \Phi_\Delta(\mathbf{1c})] / \Phi_\Delta(\mathbf{1a,1b}) \quad (7)$$

Using the data from Table 2 in toluene/pyridine (25/1), values of $\Phi_{ET}(\text{Pc}) = 0.78 \pm 0.05$ and $\Phi_{ET}(\text{Pc}) = 0.73 \pm 0.05$ were derived. From these data it was concluded that $\Phi_{ET}(\text{Pc}) = 0.75 \pm 0.05$. By combining this value with the singlet lifetime of model compound **3**, the rate constant for electron transfer from the Pc moiety was estimated as $k_{ET} = 1 \times 10^9 \text{ s}^{-1}$. Finally, the total charge-transfer quantum yield (Φ_{ET}) on excitation of the SubPc moiety in **1c** can be obtained from the contribution of both components [Eq. (8)]

$$\Phi_{ET} = \Phi_{ET}(\text{SubPc}) + \Phi_{ET}(\text{Pc}) \cdot \Phi_{EN} \quad (8)$$

which affords a value of $\Phi_{ET} = 0.9 \pm 0.1$ in the low-polarity toluene/pyridine (25/1) medium. In the more polar CH₂Cl₂, given the lower Pc fluorescence quantum yields measured (vide supra), we expect this value to be even higher. Figure 10 illustrates the deactivation pathway in dyad **1c** on SubPc or Pc excitation.

Since nanosecond transient absorption experiments failed to detect the charge-transfer state, we must conclude that charge recombination is faster than the time resolution of our experiment (ca. 20 ns). Furthermore, since the triplet quantum yield is clearly lower for dyad **1c** than for **1a** and **1b**, the radical ion pair does not recombine to a triplet state as, for example, in carotenoporphyryin-fullerene triads,^[25] but to the singlet ground state. This limits somewhat the applicability of these dyads to artificial photosynthesis or other applications where trapping of the charge-transfer state is required. Nevertheless, fine-tuning the Pc and SubPc energy levels and redox properties, as well as coupling the dyads to

Experimental Section

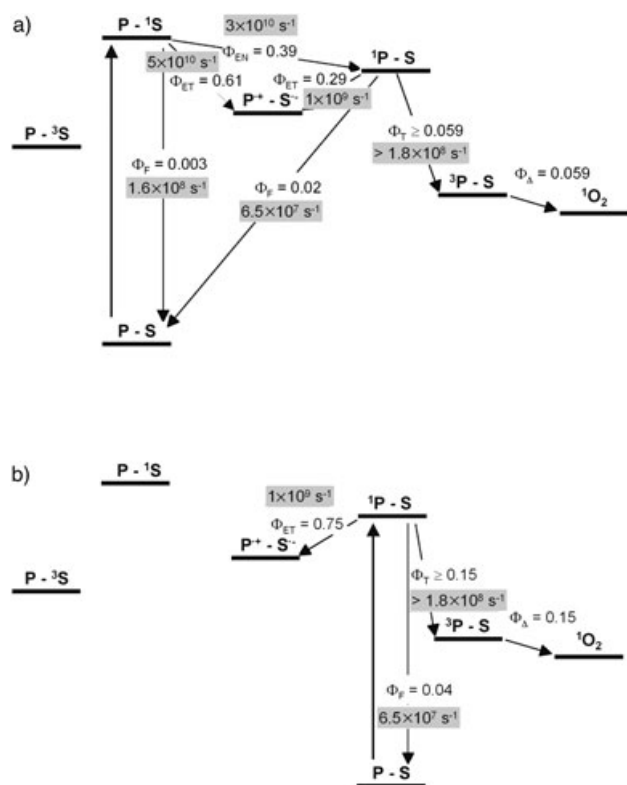


Figure 10. Photophysical processes occurring upon a) SubPc or b) Pc excitation of SubPc-Pc dyad **1c** in toluene/pyridine (25/1).

secondary electron donors or acceptors, may provide a novel route to photoactive materials.

Summary and Conclusions

We have demonstrated that subphthalocyanines and phthalocyanines are ideal partners for the construction of molecular systems able to process light. The energy level of their excited states and therefore of their optical transitions are very well suited for the efficient absorption and directional funneling, via energy-transfer processes, of photoexcitation energy. Owing to the possibility of fine-tuning the redox gap between the electron-donor and -acceptor moieties by the introduction of different substituents around the macrocyclic cores, the charge-transfer state may also be efficiently accessed via photoinduced electron-transfer processes. These features, together with the extraordinary absorptive cross section that these molecular ensembles display across the whole UV/Vis spectrum, orders of magnitude higher than those based on fullerenes and porphyrins, render them model candidates for application in situations where broad-band light sources are necessary.

General remarks: UV/Vis spectra were recorded with Hewlett-Packard 8453 and Varian Cary 4E instruments. IR spectra were recorded on a Bruker Vector 22 spectrophotometer. LSI-MS and HRMS spectra were determined on a VG AutoSpec instrument. MALDI-TOF MS spectra were recorded with a Bruker Reflex III spectrometer. NMR spectra were acquired with a Bruker AC-300 instrument. Elemental analyses were performed with a Perkin-Elmer 2400 apparatus. Column chromatography was carried out on silica gel Merck-60 (230–400 mesh, 60 Å), and TLC on aluminum sheets precoated with silica gel 60 F₂₅₄ (E. Merck). Chemicals were purchased from Aldrich Chemical Co. and used as received without further purification. 4,5-Dioctyloxyphthalonitrile,^[26] 4-(3-hydroxy-3-methyl-1-butynyl)phthalonitrile,^[27b] 4-nitrophthalonitrile,^[28] 4-iodophthalonitrile,^[27] and 4,5-dioctylthiophthalonitrile^[29] were prepared according to published procedures.

Electrochemistry: Cyclic voltammetry and Osteryoung square-wave voltammetry were performed on a Windows-driven BAS 100w electrochemical analyzer (Bioanalytical Systems, West Lafayette, IN) at room temperature with a three-electrode configuration in THF or *o*-dichlorobenzene solutions containing the substrate (typically about 0.5–1 mmol dm⁻³) and the supporting electrolyte. A glassy carbon (∅ 3 mm) disk served as the working electrode, a platinum wire (∅ 1 mm) as counterelectrode, and a commercial Ag/AgCl aqueous electrode as reference electrode. Both the counter- and the reference electrodes were directly immersed in the electrolyte solution. The surface of the working electrode was polished with commercial Alpha Micropolish Alumina No. 1C (Aldrich) with a particle size of 1.0 μm. Tetrabutylammonium hexafluorophosphate (*n*Bu₄NPF₆, Fluka, >99%) was recrystallized twice from ethanol and dried in vacuum overnight prior to use and was employed as the supporting electrolyte in 0.1 mol dm⁻³ concentration. Solutions were stirred and deaerated by bubbling argon for a few minutes prior to each voltammetric measurement. Scan rate was 100 mV s⁻¹, unless otherwise specified. OSWVs were obtained for a sweep width of 25 mV, a frequency of 15 Hz, a step potential of 4 mV, a SW amplitude of 25 mV, and a quiet time of 2 s.

Photophysics: Emission spectra were recorded with a Jobin Yvon Spex Fluoromax-2 spectrofluorometer, and the data were analyzed by the Datamax-Std. 2.20 software. A scan rate of 0.3 nm s⁻¹ and 2 nm (emission) and 1 nm (excitation) slits were employed. Fluorescence quantum yields were determined by comparing the areas under the fluorescence spectra recorded for optically matched solutions of the samples and suitable references, correcting for refractive index changes where appropriate. For the SubPc units, the range 570–650 nm was used, and for the Pc unit, 650–800 nm. Singlet-state energies were deduced from the crossing point between the normalized absorption and fluorescence spectra. Time-resolved fluorescence experiments were carried out with a fluorescence lifetime system based on the time-correlated single-photon counting technique (Edinburgh Instruments, Model FL900). The triplet-state properties, i.e., phosphorescence, transient absorption, and singlet-oxygen sensitization, were studied by nanosecond laser flash photolysis using a Continuum Surelite 10 Nd:YAG laser (355 nm, 5 ns pulse width, 100 mJ per pulse) to pump a Continuum OPO laser (410–700 nm, 5–10 mJ per pulse). Triplet- and singlet-oxygen phosphorescence was detected with a North Coast EOL-817P germanium photodiode. Transient absorption was probed by a Photon Technology International (PTI) system comprising a 75W OSRAM Xe lamp illuminator, a monochromator, and a Hamamatsu R928 photomultiplier. In each case, the output of the detector was fed to a Lecroy 9410 (150 MHz) digital oscilloscope for data acquisition and averaging and ultimately sent to a computer for storage and analysis. The triplet energy was allocated as the maximum of the near-IR emission band. The quantum yields of singlet-oxygen production were determined by comparing the singlet-oxygen phosphorescence intensity at 1270 nm recorded for optically matched solutions of the samples and suitable references in the same solvent.^[30]

The energy of the charge-transfer state (ΔG_{CS}) was estimated from the redox potentials by using Equation (9), where F is the Faraday constant, e the electron charge, ϵ_0 the permittivity of vacuum, $E(D^+/D)$ and $E(A/A^-)$ are the Pc oxidation and SubPc reduction potentials, respectively, in

the solvent considered (see below), ϵ_s is the relative permittivity of the solvent, and a the center-to-center distance between the two aromatic rings directly linked by the ethynyl spacer, taken as 6 Å.

$$\Delta G_{CS} = F[E(D^+/D) - E(A/A^-)] - \frac{Fe}{4\pi\epsilon_0\epsilon_s a} \quad (9)$$

Redox data ($E(D^+/D)$ and $E(A/A^-)$, obtained from the voltammograms in THF) were corrected for the change in solvent polarity from Equation (10), where r is the molecular radius and ϵ_{S1} and ϵ_{S2} are the relative permittivities of solvent 1 (THF) and solvent 2 (CH_2Cl_2 or toluene).

$$\Delta G_{(S1-S2)} = \frac{N_A e^2}{4\pi\epsilon_0^2} \left[\frac{1}{r} \left(\frac{1}{\epsilon_{S2}} - \frac{1}{\epsilon_{S1}} \right) \right] \quad (10)$$

From the value of $\Delta G_{(S1-S2)}$, the redox potentials in toluene or CH_2Cl_2 may be straightforwardly estimated from Equations (11) and (12).

$$E(D^+/D)_{S2} = E(D^+/D)_{S1} + \Delta G_{(S1-S2)}/F \quad (11)$$

$$E(A/A^-)_{S2} = E(A/A^-)_{S1} - \Delta G_{(S1-S2)}/F \quad (12)$$

[2,3,9,10,16,17-Hexaethyloxy-23-(3-hydroxy-3-methyl-1-butynyl)-29H,31H-phthalocyaninato(2-)- $\kappa\text{N}^{29},\kappa\text{N}^{30},\kappa\text{N}^{31},\kappa\text{N}^{32}$]zinc(II) (2): A solution of 1,2-dicyano-4,5-dioxyloxybenzene (640 mg, 1.67 mmol), 1,2-dicyano-4-(3-hydroxy-3-methyl-1-butynyl)benzene (117 mg, 0.55 mmol), and ZnCl_2 (75 mg, 0.55 mmol) in DMAE (2 mL) was stirred at reflux under an argon atmosphere for 16 h. After cooling to room temperature, the crude mixture was treated with methanol/water (1/1) and the resulting suspension was centrifuged several times. The resulting green solid was then purified by column chromatography on silica gel with CH_2Cl_2 /2-propanol (30/1) as eluent to afford phthalocyanine **2** as a green solid in 14% yield (113 mg). M.p. >250 °C; $^1\text{H NMR}$ (CDCl_3 , 300 MHz, 25 °C, TMS): δ = 8.0–7.0 (m, 9H), 4.4–3.8 (m, 12H), 2.3–1.2 (m, 72H), 1.1–0.8 ppm (m, 24H); IR (KBr): $\tilde{\nu}$ = 2931, 2853, 2154, 1606, 1460, 1384, 1278, 1049 cm^{-1} ; UV/Vis (CHCl_3): λ_{max} ($\lg(\epsilon/\text{dm}^3\text{mol}^{-1}\text{cm}^{-1})$) = 672 (5.0), 615 (4.6), 358 (4.8), 293 nm (4.7); LSI-MS (*m-NBA*): m/z : 1429 [$M+H$] $^+$; elemental analysis calcd (%) for $\text{C}_{85}\text{H}_{118}\text{N}_8\text{O}_7\text{Zn}$: C 71.43, H 8.32, N 7.84; found: C 71.80, H 8.12, N 7.34.

[2,3,9,10,16,17-hexaethyloxy-23-ethynyl-29H,31H-phthalocyaninato(2-)- $\kappa\text{N}^{29},\kappa\text{N}^{30},\kappa\text{N}^{31},\kappa\text{N}^{32}$]zinc(II) (3): A dry toluene solution (2 mL) of phthalocyanine **2** (100 mg, 0.07 mmol) and NaOH (3 mg, 0.075 mmol) was stirred under reflux in an argon atmosphere for 6 h. The solvent was removed and the solid residue was extracted with CH_2Cl_2 and washed with water. The organic phase was dried over MgSO_4 and the solvent removed. The resulting green solid was purified by column chromatography on silica gel with hexane/ethyl acetate (4/1) as eluent. Pc **3** was obtained as a green solid in 73% yield (70 mg). M.p. >250 °C; $^1\text{H NMR}$ (CDCl_3 , 300 MHz, 25 °C, TMS): δ = 8.2–7.0 (m, 9H), 4.5–3.7 (m, 12H), 2.4–0.8 ppm (m, 90H); IR (KBr): $\tilde{\nu}$ = 3306, 2923, 2853, 2110, 1604, 1495, 1460, 1384, 1279, 1049 cm^{-1} ; UV/Vis (CHCl_3): λ_{max} ($\lg(\epsilon/\text{dm}^3\text{mol}^{-1}\text{cm}^{-1})$) = 686 (4.9), 615 (4.2), 357 (4.6), 289 nm (4.3); LSI-MS (*m-NBA*): m/z : 1372 [$M+H$] $^+$. HRLSI-MS calcd for $\text{C}_{82}\text{H}_{112}\text{N}_8\text{O}_6\text{Zn}$ [M^+]: 1370.7965; found: 1370.7982; elemental analysis calcd (%) for $\text{C}_{82}\text{H}_{112}\text{N}_8\text{O}_6\text{Zn}$: C 71.83, H 8.23, N 8.17; found: C 72.22, H 7.95, N 7.89.

General procedure for the preparation of subphthalocyanines 4a–d: BCl_3 (9 mL, 1 M in *p*-xylene) was added to a mixture of 4-iodophthalonitrile (0.76 g, 3 mmol) and the corresponding phthalonitrile (6 mmol; see Scheme 1) under argon atmosphere. The reaction mixture was stirred under reflux for 30 min, allowed to reach room temperature and flushed with argon. The reaction slurry was dissolved in toluene/THF (10/1) and passed through a short silica plug. The solvent was removed by vacuum distillation and the resulting dark solid was subjected to column chromatography on silica gel with toluene/THF (100/1) (**4a**), hexane/ethyl acetate (15/1) (**4b**), toluene/THF (50/1) (**4c**), or CH_2Cl_2 /hexane (3/1) (**4d**).

Chloro[2-iodo-7,12:14,19-diimino-21,5-nitrilo-5H-tribenzo[*c,h,m*]-[1,6,11]triazacyclopentadecinato(2-)- $\kappa\text{N}^{22},\kappa\text{N}^{23},\kappa\text{N}^{24}$]-boron(III) (4a): magenta solid; 217 mg (13%); M.p. >250 °C; $^1\text{H NMR}$ (CDCl_3 , 300 MHz,

25 °C, TMS): δ = 9.26 (d, $^4J(\text{H,H})$ = 1.5 Hz, 1H), 8.95–8.85 (m, 4H), 8.61 (d, $^3J(\text{H,H})$ = 8.5 Hz, 1H), 8.22 (dd, $^3J(\text{H,H})$ = 8.5 Hz, $^4J(\text{H,H})$ = 1.5 Hz, 1H), 8.0–7.9 ppm (m, 4H); $^{13}\text{C NMR}$ (75.5 MHz, 25 °C, TMS): Owing to the low solubility of this compound, the ^{13}C signals could not be detected in any of the solvents examined (CDCl_3 , [D_6]acetone, and $\text{CDCl}_3/\text{CS}_2$ (1/2)), even after an acquisition time of 48 h; IR (KBr): $\tilde{\nu}$ = 2923, 1629, 1438, 1282, 1136, 953, 758 cm^{-1} ; UV/Vis (CHCl_3): λ_{max} ($\lg(\epsilon/\text{dm}^3\text{mol}^{-1}\text{cm}^{-1})$) = 570 (4.5), 537 (sh), 523 (sh), 309 (4.2), 272 nm (4.1); LSI-MS (*m-NBA*): m/z : 556 [M^+]; HRLSI-MS calcd for $\text{C}_{24}\text{H}_{11}\text{N}_6\text{IBCl}$ [M^+]: 555.9871, found: 555.9886; elemental analysis calcd (%) for $\text{C}_{24}\text{H}_{11}\text{N}_6\text{IBCl}$: C 51.79, H 1.99, N 15.10; found: C 51.76, H 2.06, N 15.10.

Chloro[2-iodo-9,10,16,17-tetraoctylthio-7,12:14,19-diimino-21,5-nitrilo-5H-tribenzo[*c,h,m*]-[1,6,11]triazacyclopentadecinato(2-)- $\kappa\text{N}^{22},\kappa\text{N}^{23},\kappa\text{N}^{24}$]-boron(III) (4b): greenish viscous solid; 713 mg (21%); $^1\text{H NMR}$ (CDCl_3 , 300 MHz, 25 °C, TMS): δ = 9.19 (d, $^4J(\text{H,H})$ = 1.5 Hz, 1H), 8.59 (d, $^3J(\text{H,H})$ = 8.5 Hz, 1H), 8.58 (s, 2H), 8.56 (s, 1H), 8.54 (s, 1H), 8.17 (dd, $^3J(\text{H,H})$ = 8.5 Hz, $^4J(\text{H,H})$ = 1.5 Hz, 1H), 3.4–3.1 (m, 8H), 2.0–1.8 (m, 8H), 1.7–1.5 (m, 8H), 1.5–1.2 (m, 32H), 1.0–0.8 ppm (m, 12H); $^{13}\text{C NMR}$ (CDCl_3 , 75.5 MHz, 25 °C, TMS): δ = 150.3, 150.2, 149.5, 149.3, 148.6, 147.5, 141.6, 141.5, 141.0, 140.9, 138.4, 132.0, 131.4, 129.6, 128.7, 128.4, 128.2, 128.1, 123.5, 119.7, 119.3, 119.1, 95.8, 33.7, 33.5, 31.8, 29.3, 29.2, 29.1, 28.4, 22.6, 14.1 ppm; IR (KBr): $\tilde{\nu}$ = 2954, 2924, 2852, 1596, 1461, 1419, 978, 785, 705 cm^{-1} ; UV/Vis (CHCl_3): λ_{max} ($\lg(\epsilon/\text{dm}^3\text{mol}^{-1}\text{cm}^{-1})$) = 593 (4.6), 577 (sh), 553 (sh), 429 (3.9), 357 (3.9), 309 nm (4.3); LSI-MS (*m-NBA*): m/z : 1133 [M^+]; HRLSI-MS calcd for $\text{C}_{56}\text{H}_{75}\text{N}_6\text{IS}_4\text{BCl}$ [M^+]: 1133.3841, found: 1133.3821; elemental analysis calcd (%) for $\text{C}_{56}\text{H}_{75}\text{N}_6\text{IS}_4\text{BCl}$: C 59.33, H 6.67, N 7.41, S 11.31; found: C 59.41, H 6.74, N 7.35, S 11.20.

Chloro[2-iodo-9,16-dinitro-7,12:14,19-diimino-21,5-nitrilo-5H-tribenzo[*c,h,m*]-[1,6,11]triazacyclopentadecinato(2-)- $\kappa\text{N}^{22},\kappa\text{N}^{23},\kappa\text{N}^{24}$]-boron(III) (4c): dark purple solid; 116 mg (6%); M.p. >250 °C; $^1\text{H NMR}$ (CDCl_3 , 300 MHz, 25 °C, TMS): δ = 9.76 (d, $^4J(\text{H,H})$ = 2.0 Hz, 2H), 9.28 (d, $^4J(\text{H,H})$ = 1.5 Hz, 1H), 9.06 (d, $^3J(\text{H,H})$ = 8.5 Hz, 1H), 9.00 (d, $^3J(\text{H,H})$ = 8.5 Hz, 1H), 8.83 (dd, $^3J(\text{H,H})$ = 8.8 Hz, $^4J(\text{H,H})$ = 2.0 Hz, 1H), 8.80 (dd, $^3J(\text{H,H})$ = 8.8 Hz, $^4J(\text{H,H})$ = 2.0 Hz, 1H), 8.64 (d, $^3J(\text{H,H})$ = 8.5 Hz, 1H), 8.35 ppm (dd, $^3J(\text{H,H})$ = 8.5 Hz, $^4J(\text{H,H})$ = 1.5 Hz, 1H); $^{13}\text{C NMR}$ (CDCl_3 , 75.5 MHz, 25 °C, TMS): δ = 140.3, 132.1, 125.2, 124.8, 124.2, 123.5, 119.0, 118.8, 97.9 ppm; IR (KBr): $\tilde{\nu}$ = 2922, 1617, 1525, 1440, 1342, 1317, 1261, 1183, 1097, 973, 793, 740, 647 cm^{-1} ; UV/Vis (CHCl_3): λ_{max} ($\lg(\epsilon/\text{dm}^3\text{mol}^{-1}\text{cm}^{-1})$) = 591 (4.2), 569 (4.4), 546 (4.4), 524 (4.1), 300 nm (4.3); LSI-MS (*m-NBA*): m/z : 646 [M^+]; HRLSI-MS calcd for $\text{C}_{24}\text{H}_9\text{N}_6\text{IO}_4\text{BCl}$ [M^+]: 645.9573, found: 645.9560; elemental analysis calcd (%) for $\text{C}_{24}\text{H}_9\text{N}_6\text{IO}_4\text{BCl}$: C 44.58, H 1.40, N 17.33; found: C 44.59, H 1.42, N 17.32.

Chloro[2-iodo-9,10,16,17-tetraoctylsulfonyl-7,12:14,19-diimino-21,5-nitrilo-5H-tribenzo[*c,h,m*]-[1,6,11]triazacyclopentadecinato(2-)- $\kappa\text{N}^{22},\kappa\text{N}^{23},\kappa\text{N}^{24}$]-boron(III) (4d): dark purple solid; 832 mg (22%); $^1\text{H NMR}$ (CDCl_3 , 300 MHz, 25 °C, TMS): δ = 9.9–9.75 (m, 4H), 9.31 (d, $^4J(\text{H,H})$ = 1.4 Hz, 1H), 8.64 (d, $^3J(\text{H,H})$ = 8.5 Hz, 1H), 8.42 (dd, $^3J(\text{H,H})$ = 8.5 Hz, $^4J(\text{H,H})$ = 1.4 Hz, 1H), 3.9–3.6 (m, 8H), 1.95–1.7 (m, 8H), 1.5–1.3 (m, 8H), 1.35–1.1 (m, 32H), 0.9–0.75 ppm (m, 12H); $^{13}\text{C NMR}$ (CDCl_3 , 75.5 MHz, 25 °C, TMS): δ = 153.8, 152.7, 150.2, 150.0, 147.8, 147.6, 141.1, 140.2, 140.1, 132.8, 132.6, 132.4, 131.6, 131.5, 130.5, 128.8, 128.7, 124.4, 98.9, 57.1, 31.6, 28.9, 28.2, 22.6, 22.5, 14.0 ppm; IR (KBr): $\tilde{\nu}$ = 2954, 2926, 2853, 1781, 1615, 1316, 1277, 1130, 980, 803 cm^{-1} ; UV/Vis (CHCl_3): λ_{max} ($\lg(\epsilon/\text{dm}^3\text{mol}^{-1}\text{cm}^{-1})$) = 595 (4.7), 564 (4.3), 552 (4.1), 516 (4.0), 356 (sh), 306 nm (4.3); LSI-MS (*m-NBA*): m/z : 1261 [M^+]; HRLSI-MS calcd for $\text{C}_{56}\text{H}_{75}\text{N}_6\text{IS}_4\text{O}_8\text{BCl}$ [M^+]: 1260.3355, found: 1260.3348; elemental analysis calcd (%) for $\text{C}_{56}\text{H}_{75}\text{N}_6\text{IS}_4\text{O}_8\text{BCl}$: C 53.31, H 5.99, N 6.66, S 10.16; found: C 53.45, H 6.17, N 6.55, S 10.02.

General procedure for the synthesis of subphthalocyanines 5a–c: Triethylamine (0.5 mL) was added to a dry toluene solution (2 mL) of 1-pentylene (5.5 mg, 0.081 mmol), [$\text{PdCl}_2(\text{PPh}_3)_2$] (1.5 mg, 0.0022 mmol), CuI (0.2 mg, 0.0011 mmol) and the corresponding monoiodosubphthalocyanine **4a–c** (0.054 mmol) under an argon atmosphere. The solution was stirred at room temperature for 16 (**5a**), 24 (**5b**), or 10 h (**5c**) and quenched with water. SubPc **4d** did not lead to the expected coupling compound but decomposed on addition of the base. The product was ex-

tracted with CH_2Cl_2 (3×10 mL) and the organic phases were dried over Na_2SO_4 . The solvent was removed and the resulting pink solid was purified by column chromatography on silica gel with CH_2Cl_2 /hexane (1/1) (**5a**), (1/4) (**5b**) or (3/1) (**5c**) as eluent. SubPcs **5a** and **5c** were obtained as shiny purple solids, and SubPc **5b** as a viscous dark purple solid.

Chloro[2-(1-pentynyl)-7,12:14,19-diimino-21,5-nitrile-5H-tribenzo[*c,h,m*]-[1,6,11]triazacyclopentadecinato(2-)- $\kappa\text{N}^{22},\kappa\text{N}^{23},\kappa\text{N}^{24}$]boron(III) (5a**):** 21 mg (78 %); m.p. > 250 °C; $^1\text{H NMR}$ (CDCl_3 , 300 MHz, 25 °C, TMS): δ = 8.92 (s, 1H), 8.95–8.85 (m, 4H), 8.78 (dd, $^3J(\text{H,H})$ = 8.1 Hz, $^4J(\text{H,H})$ = 2.2 Hz, 1H), 8.0–7.9 (m, 5H), 2.51 (t, $^3J(\text{H,H})$ = 6.9 Hz, 2H), 1.73 (h, $^3J(\text{H,H})$ = 7.3 Hz, 2H), 1.13 ppm (t, $^3J(\text{H,H})$ = 7.3 Hz, 3H); $^{13}\text{C NMR}$ (CDCl_3 , 75.5 MHz, 25 °C, TMS): δ = 150.2, 150.0, 149.9, 149.4, 149.3, 133.1, 131.13, 131.08, 131.0, 130.2, 130.1, 129.3, 126.3, 125.5, 122.4, 122.1, 93.8, 80.8, 22.1, 21.6, 13.6 ppm; UV/Vis (CHCl_3): λ_{max} ($\lg(\epsilon/\text{dm}^3\text{mol}^{-1}\text{cm}^{-1})$) = 573 (4.5), 527 (sh), 308 (4.0), 273 nm (4.0); LSI-MS (*m*-NBA): *m/z*: 497 [*M*] $^+$; HRLSI-MS calcd for $\text{C}_{29}\text{H}_{18}\text{N}_6\text{BCl}$ [*M*] $^+$: 496.1374, found: 496.1345; Elemental analysis calcd (%) for $\text{C}_{29}\text{H}_{18}\text{N}_6\text{BCl}$: C 70.12, H 3.65, N 16.92; found: C 70.17, H 3.66, N 16.97.

Chloro[2-(1-pentynyl)-9,10,16,17-tetraoctylthio-7,12:14,19-diimino-21,5-nitrilo-5H-tribenzo[*c,h,m*]-[1,6,11]triazacyclopentadecinato(2-)- $\kappa\text{N}^{22},\kappa\text{N}^{23},\kappa\text{N}^{24}$]boron(III) (5b**):** 32 mg (54 %); $^1\text{H NMR}$ (CDCl_3 , 300 MHz, 25 °C, TMS): δ = 8.89 (s, 1H), 8.74 (d, $^3J(\text{H,H})$ = 8.6 Hz, 1H), 8.6–8.5 (m, 4H), 7.90 (d, $^3J(\text{H,H})$ = 8.5 Hz, 1H), 3.4–3.1 (m, 8H), 2.52 (t, $^3J(\text{H,H})$ = 7.0 Hz, 2H), 1.9–1.2 (m, 50H), 1.14 (t, $^3J(\text{H,H})$ = 7.2 Hz, 3H), 0.8 ppm (m, 12H); UV/Vis (CHCl_3): λ_{max} ($\lg(\epsilon/\text{dm}^3\text{mol}^{-1}\text{cm}^{-1})$) = 595 (4.6), 580 (sh), 553 (sh), 422 (4.1), 363 (4.3), 305 nm (4.6); LSI-MS (*m*-NBA): *m/z*: 1074 [*M+H*] $^+$; HRLSI-MS calcd for $\text{C}_{61}\text{H}_{83}\text{N}_6\text{S}_4\text{BCl}$ [*M+H*] $^+$: 1072.5265, found: 1072.5301; elemental analysis calcd (%) for $\text{C}_{61}\text{H}_{82}\text{N}_6\text{S}_4\text{BCl}$: C 68.23, H 7.70, N 7.83; found: C 68.37, H 7.96, N 7.76.

Chloro[2-(1-pentynyl)-9,16-dinitro-7,12:14,19-diimino-21,5-nitrilo-5H-tribenzo[*c,h,m*]-[1,6,11]triazacyclopentadecinato(2-)- $\kappa\text{N}^{22},\kappa\text{N}^{23},\kappa\text{N}^{24}$]boron(III) (5c**):** 28 mg (88 %); M.p. > 250 °C; $^1\text{H NMR}$ (CDCl_3 , 300 MHz, 25 °C, TMS): δ = 9.76–9.74 (m, 2H), 9.02 (d, $^3J(\text{H,H})$ = 8.5 Hz, 1H), 9.00 (d, $^3J(\text{H,H})$ = 8.5 Hz, 1H), 8.92 (s, 1H), 8.85–8.7 (m, 3H), 8.03 (dd, $^3J(\text{H,H})$ = 8.1 Hz, $^4J(\text{H,H})$ = 1.3 Hz, 1H), 2.53 (t, $^3J(\text{H,H})$ = 7.2 Hz, 2H), 1.74 (h, $^3J(\text{H,H})$ = 7.2 Hz, 2H), 1.14 ppm (t, $^3J(\text{H,H})$ = 7.2 Hz, 3H); $^{13}\text{C NMR}$ ($[\text{D}_6]$ acetone, 75.5 MHz, 25 °C, TMS): δ = 153.8, 153.6, 152.4, 150.8, 150.7, 150.0, 148.6, 148.5, 134.3, 134.2, 133.6, 130.7, 130.3, 130.0, 126.8, 124.8, 124.4, 124.0, 123.0, 122.9, 122.4, 117.8, 117.6, 80.5, 61.1, 22.0, 21.1, 13.0 ppm; UV/Vis (CHCl_3): λ_{max} ($\lg(\epsilon/\text{dm}^3\text{mol}^{-1}\text{cm}^{-1})$) = 596 (4.6), 573 (4.5), 551 (4.3), 527 (4.2), 296 (4.4), 274 (4.5), 246 nm (4.4); LSI-MS (*m*-NBA): *m/z*: 587 [*M*] $^+$; HRLSI-MS calcd for $\text{C}_{29}\text{H}_{16}\text{N}_8\text{O}_2\text{BCl}$ [*M*] $^+$: 586.1076, found: 586.1075; elemental analysis calcd (%) for $\text{C}_{29}\text{H}_{16}\text{N}_8\text{O}_2\text{BCl}$: C 59.36, H 2.75, N 19.10; found: C 59.41, H 2.79, N 19.04.

General procedure for the synthesis of SubPc–Pc dyads 1a–c: Freshly distilled triethylamine (0.5 mL) was added to a dry toluene solution of monoalkynylphthalocyanine **3** (40 mg, 0.03 mmol), $[\text{PdCl}_2(\text{PPh}_3)_2]$ (1 mg, 0.0014 mmol), CuI (0.2 mg, 0.001 mmol), and the corresponding monoiodosubphthalocyanine **4a–d** (0.026 mmol) under an argon atmosphere. The mixture was stirred for 8 h (**1a**), 16 h (**1b**) or 3 h (**1c**) at room temperature, quenched with water and extracted with CH_2Cl_2 (3×10 mL). SubPc **4d** did not lead to the expected coupling compound but decomposed on addition of the base. The combined organic layers were dried over Na_2SO_4 . After removal of the solvent the greenish blue solid was purified by column chromatography on silica gel with CHCl_3 /ethyl acetate (40/1) and then hexane/dioxane (4/1) as eluents for **1a**, CHCl_3 /ethyl acetate (50/1) and then hexane/dioxane (6/1) as eluents for **1b** and CHCl_3 /ethyl acetate (40/1) and then hexane/dioxane (4/1) as eluents for **1c**.

Subphthalocyanine–phthalocyanine dyad 1a: Intense blue solid; 26 mg (53 %); m.p. > 250 °C; $^1\text{H NMR}$ (CDCl_3 , 300 MHz, 25 °C, TMS): δ = 9.0–8.5, 8.0–7.5 (m, 20H), 4.2–3.3 (m, 12H), 2.2–1.3 (m, 72H), 1.1–0.8 ppm (m, 18H); IR (KBr): $\tilde{\nu}$ = 2923, 2853, 2208, 1605, 1495, 1460, 1384, 1280, 1092, 1048, 973, 796 cm^{-1} ; UV/Vis (CHCl_3): λ_{max} ($\lg(\epsilon/\text{dm}^3\text{mol}^{-1}\text{cm}^{-1})$) = 698 (4.8), 677 (4.8), 641 (4.2), 617 (4.2), 578 (4.5), 528 (sh), 357 (4.7), 298 nm (4.6); MALDI-TOF MS (dithranol): *m/z*: 1796–1806 [*M*] $^+$ (see isotopic pattern in the Supporting Information); elemental analysis calcd

(%) for $\text{C}_{106}\text{H}_{122}\text{N}_{14}\text{O}_6\text{BClZn}$: C 70.74, H 6.83, N 10.89; found: C 71.26, H 6.44, N 10.22.

Subphthalocyanine–phthalocyanine dyad 1b: Green viscous solid; 28 mg (45 %); $^1\text{H NMR}$ (CDCl_3 , 300 MHz, 25 °C, TMS): δ = 9.0–8.5, 8.0–7.5 (m, 16H), 4.2–2.9 (m, 20H), 2.2–1.3 (m, 120H), 1.1–0.8 ppm (m, 30H); IR (KBr): $\tilde{\nu}$ = 2954, 2924, 2852, 2208, 1597, 1456, 1280, 1092, 1048, 977, 785, 706 cm^{-1} ; UV/Vis (CHCl_3): λ_{max} ($\lg(\epsilon/\text{dm}^3\text{mol}^{-1}\text{cm}^{-1})$) = 701 (4.9), 677 (4.9), 656 (4.4), 597 (4.6), 426 (sh), 357 (4.8), 296 nm (4.7); MALDI-TOF MS (dithranol): *m/z*: 2372–2382 [*M*] $^+$ (for isotopic pattern, see Supporting Information); elemental analysis calcd (%) for $\text{C}_{138}\text{H}_{186}\text{N}_{14}\text{O}_6\text{S}_2\text{BClZn}$: C 69.73, H 7.89, N 8.25; found: C 70.28, H 7.21, N 8.04.

Subphthalocyanine–phthalocyanine dyad 1c: Greenish blue solid; 34 mg (69 %); m.p. > 250 °C; $^1\text{H NMR}$ (CDCl_3 , 300 MHz, 25 °C, TMS): δ = 9.5–9.0, 8.0–7.0 (m, 18H), 4.2–3.5 (m, 12H), 2.0–1.1 (m, 72H), 1.1–0.8 ppm (m, 18H); IR (KBr): $\tilde{\nu}$ = 2924, 2854, 2200, 1605, 1529, 1494, 1459, 1384, 1339, 1279, 1093, 1048, 970, 797 cm^{-1} ; UV/Vis (CHCl_3): λ_{max} ($\lg(\epsilon/\text{dm}^3\text{mol}^{-1}\text{cm}^{-1})$) = 702 (4.9), 678 (5.0), 654 (sh), 594 (4.6), 586 (sh), 557 (sh), 538 (sh), 361 (4.8), 298 nm (4.8); MALDI-TOF MS (dithranol): *m/z*: 1885–1895 [*M*] $^+$ (for isotopic pattern, see Supporting Information); elemental analysis calcd (%) for $\text{C}_{106}\text{H}_{120}\text{N}_{16}\text{O}_{10}\text{BClZn}$: C 67.37, H 6.40, N 11.86; found: C 67.80, H 6.05, N 11.45.

Acknowledgements

The authors are grateful for the financial support of the CICYT (Spain), Comunidad de Madrid and the European Union through grants BQU2002-04697, 07N/0030/2002, and HPRN-CT-2000-00020 (T.T.). This work was also partially supported by the U.S. National Science Foundation, grant CHE-0135786 (L.E.), and the Office of Basic Energy Sciences of the U.S. Financial support by the Spanish MCYT, ref SAF 2002-04034-C02-2 is gratefully acknowledged (S.N.). We are indebted to Professor Silvia E. Braslavsky, Max-Planck-Institut für Bioorganische Chemie, for the fluorescence lifetime measurements.

- [1] a) *Photoinduced Electron Transfer* (Eds.: M. A. Fox, M. Chanon), Elsevier, Amsterdam, **1988**; b) V. Balzani, F. Scandola, *Supramolecular Photochemistry*, Ellis Horwood, Chichester, **1991**, pp. 161–196, 355–394; c) S. Speiser, *Chem. Rev.* **1996**, *96*, 1953–1976; d) J. G. Calbert, *Photochemistry*, Wiley, New York, **1996**; e) D. Gust, *Nature* **1997**, *386*, 21–22; f) *Electron Transfer in Chemistry, Vols. I–V* (Ed.: V. Balzani), Wiley-VCH, Weinheim, **2001**.
- [2] a) G. Feher, J. P. Allen, M. Y. Okamura, D. C. Rees, *Nature* **1989**, *339*, 111–116; b) R. Huber, *Angew. Chem.* **1989**, *101*, 849–871; *Angew. Chem. Int. Ed. Engl.* **1989**, *28*, 849–871; c) J. Deisenhofer, H. Michel, *Angew. Chem.* **1989**, *101*, 872–892; *Angew. Chem. Int. Ed. Engl.* **1989**, *28*, 872–892; d) *The Photosynthetic Reaction Center* (Eds.: J. Deisenhofer, J. R. Norris), Academic Press, New York, **1993**; e) *Molecular Mechanisms of Photosynthesis* (Ed.: R. E. Blankenship), Blackwell Science, **2002**.
- [3] a) M. R. Wasielewski, *Chem. Rev.* **1992**, *92*, 435–461; b) D. Gust, T. A. Moore, A. L. Moore, *Acc. Chem. Res.* **1993**, *26*, 198–205; c) H. Kurreck, M. Huber, *Angew. Chem.* **1995**, *107*, 929–947; *Angew. Chem. Int. Ed. Engl.* **1995**, *34*, 849–866; d) D. Gust, T. A. Moore, A. L. Moore, *Acc. Chem. Res.* **2001**, *34*, 40–48; e) M. Huber, *Eur. J. Org. Chem.* **2001**, *23*, 4379–4389.
- [4] Such is the case, for instance, for C_{60} fullerene, which affords lower reorganization energies than quinones or other planar electron-accepting units: H. Imahori, H. Yamada, D. M. Guldi, Y. Endo, A. Shimomura, S. Kundu, K. Yamada, T. Okada, Y. Sakata, S. Fukuzumi, *Angew. Chem.* **2002**, *114*, 2450–2453; *Angew. Chem. Int. Ed.* **2002**, *41*, 2344–2347.
- [5] a) *Phthalocyanines. Properties and Applications, Vols. I–4* (Eds.: C. C. Leznoff, A. B. P. Lever), VCH Publishers, Cambridge, **1989**, **1993**, **1996**; b) *Phthalocyanine Materials. Synthesis, Structure and*

- Function* (Ed.: N. B. McKeown), Cambridge University Press, Cambridge, **1998**; c) G. de la Torre, M. Nicolau, T. Torres in *Supramolecular Photosensitive and Electroactive Materials* (Ed.: H. S. Nalwa), Academic Press, New York, **2001**, pp. 1–111; d) *The Porphyrin Handbook, Vols. 15–20* (Eds.: K. M. Kadish, K. M. Smith, R. Guillard), Academic Press, San Diego, **2003**.
- [6] C. G. Claessens, D. González-Rodríguez, T. Torres, *Chem. Rev.* **2002**, *102*, 835–853.
- [7] a) S. Ho Kang, Y.-S. Kang, W.-C. Zin, G. Olbrechts, K. Wostyn, K. Clays, A. Persoons, K. Kim, *Chem. Commun.* **1999**, 1661–1662; b) C. G. Claessens, T. Torres, *J. Am. Chem. Soc.* **2002**, *124*, 14522–14523; c) C. G. Claessens, T. Torres, *Chem. Commun.* **2004**, 1298–1299.
- [8] a) B. del Rey, U. Keller, T. Torres, G. Rojo, F. Agulló-López, S. Nonell, C. Martí, S. Brasselet, I. Ledoux, J. Zyss, *J. Am. Chem. Soc.* **1998**, *120*, 12808–12817; b) G. Martín, G. Rojo, F. Agulló-López, V. R. Ferro, J. M. García de la Vega, M. V. Martínez-Díaz, T. Torres, I. Ledoux, J. Zyss, *J. Phys. Chem. B* **2002**, *106*, 13139–13145; c) C. G. Claessens, D. González-Rodríguez, T. Torres, G. Martín, F. Agulló-López, I. Ledoux, J. Zyss, V. R. Ferro, J. M. García de la Vega, *J. Phys. Chem. B*, **2005**, *109*, 3800–3806.
- [9] a) D. González-Rodríguez, T. Torres, D. M. Guldi, J. Rivera, L. Echegoyen, *Org. Lett.* **2002**, *4*, 335–338; b) D. González-Rodríguez, T. Torres, M. A. Herranz, J. Rivera, L. Echegoyen, D. M. Guldi, *J. Am. Chem. Soc.* **2004**, *126*, 6301–6313.
- [10] For some recent examples of Pc-based systems, see: a) E. Mariño-Ochoa, R. Palacios, G. Kodis, A. N. Macpherson, T. Gillbro, D. Gust, A. L. Moore, T. A. Moore, *Photochem. PhotoBiophys.* **2002**, *76*, 116–121; b) C. Farren, C. A. Christensen, S. FitzGerald, M. R. Bryce, A. Beeby, *J. Org. Chem.* **2002**, *67*, 9130–9139; c) D. M. Guldi, A. Gouloumis, P. Vázquez, T. Torres, *Chem. Commun.* **2002**, 2056–2057; d) D. M. Guldi, J. Ramey, M. V. Martínez-Díaz, A. de la Escosura, T. Torres, T. Da Ros, M. Prato, *Chem. Commun.* **2002**, 2774–2775; e) D. González-Rodríguez, T. Torres in *The Exciting World of Nanocages and Nanotubes* (Eds.: P. Kamat, D. M. Guldi, K. Kadish), *Proc. Electrochem. Soc., Fullerenes Vol. 12*, ECS, Pennington NJ, **2002**, pp. 195–210; f) A. González, C. G. Claessens, G. Martín, I. Ledoux, P. Vázquez, J. Zyss, F. Agulló-López, T. Torres, *Synth. Met.* **2003**, *137*, 1487–1488; g) A. González, P. Vázquez, T. Torres, D. M. Guldi, *J. Org. Chem.* **2003**, *68*, 8635–8642; h) A. Gouloumis, D. González-Rodríguez, P. Vázquez, T. Torres, S.-G. Liu, L. Echegoyen, J. Ramey, D. M. Guldi, *J. Am. Chem. Soc.*, submitted.
- [11] a) N. Kobayashi, *J. Chem. Soc. Chem. Commun.* **1991**, 1203–1205; b) R. A. Kipp, J. A. Simon, M. Beggs, H. E. Ensley, R. H. Schmehl, *J. Phys. Chem. A* **1998**, *102*, 5659–5664; c) S. Nonell, N. Rubio, B. del Rey, T. Torres, *J. Chem. Soc. Perkin Trans. 2* **2000**, 1091–1094; d) D. Wrobel, A. Boguta, P. Mazurkiewicz, *Spectrochim. Acta Part A* **2003**, *12*, 2841–2854.
- [12] Similar porphyrin–phthalocyanine dyads have been recently described: a) S. I. Yang, J. Li, H. S. Cho, D. Kim, D. F. Bocian, D. Holten, J. S. Lindsey, *J. Mater. Chem.* **2000**, *10*, 283–296; b) M. A. miller, R. K. Lammi, S. Prathapan, D. Holten, J. S. Lindsey, *J. Org. Chem.* **2000**, *65*, 6634–6649; c) A. Ambroise, R. W. Wagner, P. D. Rao, J. A. Riggs, P. Hascoat, J. R. Diers, J. Seth, R. K. Lammi, D. F. Bocian, D. Holten, J. S. Lindsey, *Chem. Mater.* **2001**, *13*, 1023–1034.
- [13] a) G. de la Torre, C. G. Claessens, T. Torres, *Eur. J. Org. Chem.* **2000**, 2821–2830; b) T. Torres, *J. Porphyrins Phthalocyanines* **2000**, *4*, 325–330; c) G. de la Torre, T. Torres, *J. Porphyrins Phthalocyanines* **2002**, *6*, 274–284.
- [14] C. G. Claessens, T. Torres, *Chem. Eur. J.* **2000**, *6*, 2168–2172.
- [15] a) E. M. Maya, C. García, E. M. García-Frutos, P. Vázquez, T. Torres, *J. Org. Chem.* **2000**, *65*, 2733–2739; b) E. M. García-Frutos, F. Fernández-Lázaro, E. M. Maya, P. Vázquez, T. Torres, *J. Org. Chem.* **2000**, *65*, 6841–6846.
- [16] D. E. Ames, D. Bull, C. Takundwa, *Synthesis* **1981**, 364–365.
- [17] C. G. Claessens, D. González-Rodríguez, T. Torres, G. Mark, H.-P. Schuchmann, C. von Sonntag, J. Lye, J. G. MacDonald, R. S. Nohr, *Eur. J. Org. Chem.* **2003**, 2547–2551.
- [18] The complete characterization of the different isomers formed in these reactions will be published elsewhere.
- [19] a) E. M. Maya, P. Vázquez, T. Torres, *Chem. Eur. J.* **1999**, *5*, 2004–2013; b) E. M. Maya, P. Vázquez, T. Torres, L. Gobbi, F. Diederich, S. Pyo, L. Echegoyen, *J. Org. Chem.* **2000**, *65*, 823–830.
- [20] N. Kobayashi, H. Ogata, *Eur. J. Inorg. Chem.* **2004**, 906–914, and references therein.
- [21] S. L. Murov, I. Carmichael, G. L. Hug, *Handbook of Photochemistry*, Marcel Dekker, New York, **1993**, p. 1–420.
- [22] D. Magde, J. H. Brannon, T. L. Cremers, J. Olmsted III, *J. Phys. Chem.* **1979**, *83*, 696–699.
- [23] N. Kobayashi, M. Togashi, T. Osa, K. Ishii, S. Yamauchi, H. Hino, *J. Am. Chem. Soc.* **2002**, *124*, 1073–1085.
- [24] J. W. Arbogast, A. P. Darmany, C. S. Foote, Y. Rubin, F. N. Diederich, M. M. Alvarez, S. J. Anz, R. L. Whetten, *J. Phys. Chem.* **1991**, *95*, 11.
- [25] D. Kuciauskas, P. A. Liddell, S. Lin, S. G. Stone, A. L. Moore, T. A. Moore, D. Gust, *J. Phys. Chem. B* **2000**, *104*, 4307–4321.
- [26] J. F. van der Pol, E. Neeleman, J. W. Zwikker, R. J. M. Nolte, W. Drenth, *Recl. Trav. Chim. Pays-Bas* **1988**, *107*, 615–620.
- [27] a) J. Griffiths, B. Roozpekar, *J. Chem. Soc. Perkin Trans. 1* **1976**, 42–45; b) M. S. Marcuccio, I. Polina, S. Greenberg, A. B. P. Lever, C. C. Leznoff, B. Tomer, *Can. J. Chem.* **1985**, *63*, 3057–3069.
- [28] J. G. Young, W. Onyebuagu, *J. Org. Chem.* **1990**, *55*, 2155–2159.
- [29] a) D. Wöhrle, M. Eskes, K. Shigehara, A. Yamada, *Synthesis* **1993**, 194–196; b) A. Gürek, Ö. Bekaroglu, *J. Chem. Soc. Dalton Trans.* **1994**, 1419–1423.
- [30] S. Nonell, S. E. Braslavsky in *Singlet Oxygen, UV-A and Ozone* (Eds.: L. Packer, H. Sies), *Methods in Enzymology*, **2000**, *319*, 37–49.

Received: July 29, 2004

Revised: January 18, 2005

Published online: April 13, 2005